

Single-Dye NIR-II Chemiluminescence System for H₂O₂ Imaging

Zong Chang^{1#}, Chenchen Liu^{1,2#}, Like Guo, Bingxin Shu¹, Huageng Liang^{2*}, Jie Ding^{3*}, Xiaoping Zhang^{2*}, Qincao Sun^{1*}

¹Guangdong Provincial Key Laboratory of Biomedical Optical Imaging Technology & Center for Biomedical Optics and Molecular Imaging, Shenzhen Institute of Advanced Technology, Chinese Academy of Sciences, Shenzhen 518055, China.

²Department of Urology, Union Hospital, Tongji Medical College, Huazhong University of Science and Technology, Wuhan 430022, China

³Green Catalysis Center, College of Chemistry, Zhengzhou University, Zhengzhou 450000, China

Experimental Section

Materials

All reagents and solvents were used as received without further purification bovine serum albumin (BSA) (98%) were purchased from Sigma-Aldrich (St. Louis, USA). Roswell Park Memorial Institute 1640 (RPMI 1064) Medium and Penicillin–Streptomycin was purchased from HyClone. Phosphate-buffered solution (PBS) was purchased from Corning. Pancreatin was purchased from Coolaber. Dulbecco's Modified Eagle's Medium (DMEM) and fetal bovine serum (FBS) were purchased from Gibco. ZnO nanoparticles 30 nm in aqueous solution, ZnSO₄, NaOH, H₂O₂ 30%, IR26 and all other chemicals were bought from Aladdin (Shanghai, China). Glucose oxidase from *Aspergillus niger* lyophilized powder, 100,000-250,000 units/g, Dioctyl sebacate (DOS), Triton X-100, bis(2,4,5-trichloro-6-carboxyphenyl) oxalate (CPPO) were purchased from Sigma-Aldrich. Deionized water (18.25 MΩ cm, 25 °C; Millipore, Billerica, USA) was used for all experiments. Flash chromatography was performed on columns of silica gel (300–400 mesh) supplied by Yantai Silica Gel Factory (China). ONOO⁻ was prepared by mixing working solution of 1 mL 0.5 M H₂O₂, 1 mL 0.3 M HCl and 1 mL 0.1 M NaNO₂ was mixed and then 1 mL 2 M NaOH was added, the concentration of ONOO⁻ was adjusted to 1.5 mM by the absorption at 298 nm (1670 M⁻¹ cm⁻¹). ClO⁻ (1.5 mM) was prepared by diluting commercial NaClO solution in deionized water. •OH was generated from the online reaction of FeSO₄ (1.5 mM) and H₂O₂ (1.5 mM) through the Fenton reaction.

Instruments

¹H spectra were recorded on Bruker spectrometers operating at 400 MHz for 1H. For ¹H NMR spectra, chemical shifts (δ) are reported in parts per million (ppm) with reference to tetramethylsilane (δ = 0.00 ppm) or residual protonated solvent (δ = 7.26 ppm for CHCl₃, δ = 3.31 ppm for CHD₂OD) as internal standards. Splitting patterns for ¹H signals are designated as s (singlet), d (doublet), t (triplet), q (quartet), m (multiplet) and coupling constants (J) are reported in Hz. The UV-Vis-NIR absorption spectra were recorded on UV-2700 or UV-3600 Spectrophotometer (SHIMADZU, Japan). High-resolution mass spectrometry (HRMS) data were recorded using matrix-assisted laser desorption ionization time-of-flight mass spectrometer (MALDI-TOF MS) (Bruker New ultrafleXtreme) in positive mode. Powder X-ray diffraction (XRD) were recorded on a Bruker D8 ADVANCE X diffractometer employing within 2θ in the range of 10–80° and Cu Kα radiation (λ=1.54156Å) at a scan rate of 4 degree/min. Dynamic light scattering was measured by the Malvern Zetasizer. The emission spectra were measured by a calibrated InGaAs detector (Edinburgh Instruments FLS920). For chemiluminescence in wavelength range from 800 nm to 1200 nm, Edinburgh Instruments FLS920 was used. For chemiluminescence range from 300 nm to 900 nm, a TECAN Infinite M1000 PRO was used. For Transmission electron microscopy (TEM) imaging, FEI Talos F200X Super X was used with a field emission transmission electron microscope operated at 200 kV.

Abbreviations

CIEEL: chemically initiated electron exchange luminescence; DOD: 1,2-dioxetanedione; CRET: chemiluminescence resonance energy transfer; QY: quantum yield; LUMO: lowest unoccupied molecular orbital; HOMO: highest occupied molecular orbital; LUMO_{DOD}: LUMO orbital of DOD; HOMO_{Dye}: HOMO of dye. FDA: Food and Drug Administration of US; ICG: Indocyanine Green; BSA: Bovine Serum Albumin; BSAZn: the prepared nanoparticle with BSA; NIR-II: Second Near Infrared Window.

C.L. Nanoparticle preparation

Generally, 40 μL or 160 μL Q842/Q995 (10 mg/ml) in THF solution, 80 μL CPPO (50 mg/mL) in THF, 80 μL Triton X-100 and 16 μL DOS was mixed first and then added to 4 mL H₂O drop by drop. The THF was blown away via N₂ flow and the final solution volume was adjusted back to 4 mL. The final mass concentration of Q842/Q995 was about 0.1 mg/mL or 0.4 mg/mL and of CPPO was about 1 mg/mL.

BSAZn Nanoenzyme preparation

1. The precipitate of 30 mg ZnCl₂ in 1 ml water was washed with water by centrifugation for 6 times to reach a pH around 7. Then 150 mg BSA in 1.5 ml milliQ H₂O was added to the washed precipitate, sonication bath for 5 mins and then incubated for overnight under gentle shaking. In the end, a clear solution was obtained via passing through a 220 nm filter.

2. 30 mg ZnSO₄ in 1 ml water was mixed with 4 ml 0.1M NaOH solution to obtain white precipitate. It was washed with water by centrifugation for 6 times to reach a pH around 7. Then 150 mg BSA in 1.5 ml milliQ H₂O was added to the washed precipitate, sonication bath for 5 mins and then incubated for overnight under gentle shaking. In the end, a clear solution was obtained via passing through a 220 nm filter.

Relative fluorescence quantum yield.

The ICG in MeOH (QY=7.8%) solution was used as reference for IR785, Q842 and Q995 in THF with 10% H₂O with excitation wavelength about 785 nm. Five solutions with different absorbance (lower than 0.1) were prepared for reference dye and the fluorophores at 785 nm. The calculation of QY of Q842 as an example. A linear fitting was applied to both Q842 and ICG as a function of absorbance. The relative quantum yield of SQN2 was calculated in following equation:

$$\frac{QY_{Q825}}{QY_{ICG}} = \frac{n_{solvent}^2}{n_{MeOH}^2} \times \frac{Slope_{Q825}}{Slope_{ICG}}$$

The refractive index of THF (1.4) with 10% H₂O (1.3) is taken as 1.4, and that of MeOH is taken as 1.3. The slope is from the linear fitting function of corresponding fluorophores. Same procedure was applied for the measurement of all other measurements. For Q1044, Q1086 and IR26, the Q995 was used as a QY reference with excitation wavelength at 958 nm. The Errors were calculated with three groups of QY measurements.

NIR-II chemiluminescence imaging setup

A home-built cooling system was used to deep cooling an InGaAs camera (650 x 512 pixels, Tekwin, designed with cooling temperature -10 °C) to -30 °C, the gain was set to high, and different exposure times were used to achieve sufficient signal and frame rates. A single lens system was used to focus the image on camera. Fiji was used for all image treatments.

Cellular culture

The human cervical cancer cell line (Hela cells) was maintained in the DMEM medium. Both media were supplemented with 10% FBS and 1% (v/v) penicillin–streptomycin. The culture environment was 37 °C, and the humidification condition was 5% CO₂.

Mouse tumor model

All animal handling and experimental procedures were approved by Shenzhen Institutes of Advanced Technology, with case number of SIAT-IACUC-200407-YGS-SQC-A1257 and were performed in compliance with the Animal Study Committee of the Shenzhen Institutes of Advanced Technology, Chinese Academy of Sciences. All BALB/c mice were purchased from Beijing Vital River Laboratory Animal Technology Co. Ltd. During all experiments, mice were kept under anesthesia using 1.5% isoflurane mixed with pure oxygen and the body temperature was maintained at 37.5 °C by using a heating pad. 8 weeks old BALB/c mice were used for tumor implantation. Hela cells were incubated with RPMI 1640 medium (10% FBS and 1% penicillin-streptomycin). The incubated Hela cells (about 1 x 10⁶) were suspended in 100 μL 1x PBS and then inoculated subcutaneously into the posterior flank of mouse right hindlimb under full anesthesia. After about two weeks, the inoculated cells grew up to a lump with a diameter about 3 mm.

DFT calculation

Density functional theory (DFT) has been applied to the optimization of the ground state of all molecules in the singlet state. The calculation was performed using Becke's three-parameter exchange functional¹ combined with the Lee–Yang–Parr correlation functional² (B3LYP) at the level of 6-311G. The frequency calculations performed on the optimized geometries showed that they all correspond to real minima (no imaginary frequencies). The transition state was identified as one imaginary frequency. All calculations were performed in Gaussian16 program.³

```
O      1.68167900 -1.01106100  0.00001900
O      -1.68168200 -1.01105700 -0.00002000
The Cartesian Coordinate of DOD
C      0.73347500 -0.24248300  0.00000300
C      -0.76356500 -0.24248100 -0.00000400
O      -0.78693900  1.19292100 -0.00002100
O      0.78694400  1.19292000  0.00002200
```

```
The Cartesian Coordinate of DOD@TS
O      -1.34549100  1.11321000 -0.00000100
O      1.34534500  1.11331300  0.00000100
C      0.73347500 -0.00001500  0.00000000
C      -0.73353700 -0.00003000  0.00000000
O      1.34562200 -1.11315900 -0.00000100
```

O -1.34542900 -1.11333000 0.00000100

The Cartesian Coordinate of DOD@D with Frozen C-C Bond

O 1.12508500 0.93819000 -0.71262400
O -1.12583100 -0.71269100 -0.93768500
C -0.88340200 -0.00002200 0.00006000
C 0.88360800 -0.00002000 -0.00019900
O -1.12543300 0.71244200 0.93812300
O 1.12602400 -0.93790900 0.71228900

B 3 4 F

The Cartesian Coordinate of CO₂

O -1.34549100 1.11321000 -0.00000100
O 1.34534500 1.11331300 0.00000100
C 0.73347500 -0.00001500 0.00000000
C -0.73353700 -0.00003000 0.00000000
O 1.34562200 -1.11315900 -0.00000100
O -1.34542900 -1.11333000 0.00000100

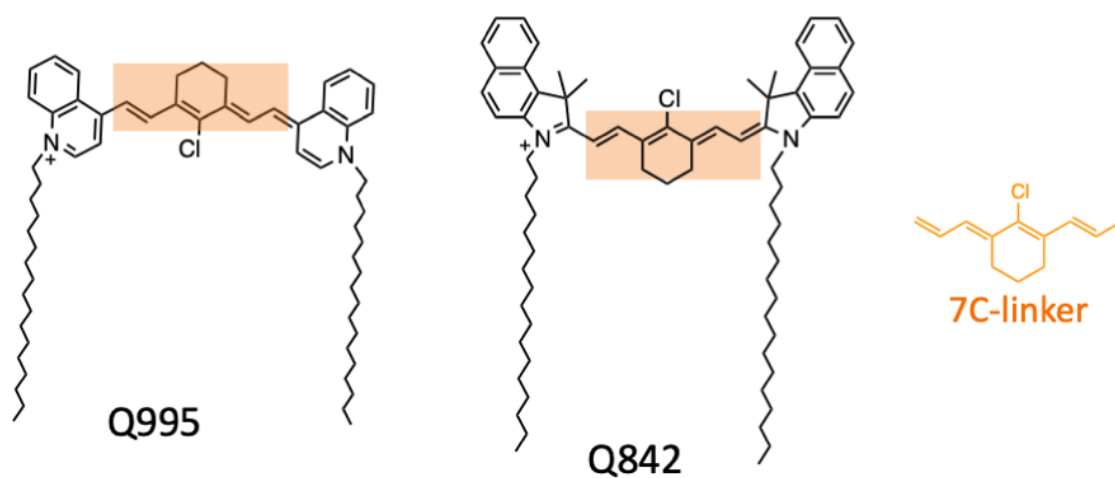


Figure S1. Molecular structures of the Q995 and Q842 dyes.

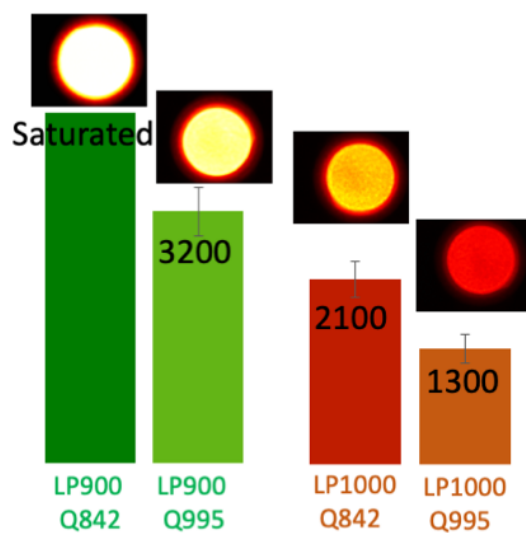


Figure S2. The chemiluminescence of Q842 and Q995 in THF with different long pass filters of 900 nm and 1000 nm. Exposure time 1s, molar concentration of Q842 and Q995 about $0.3 \mu\text{mol/mL}$, CPPO about 1 mg/mL , H_2O_2 about 100 mM , 2.5 mM of NaOH.

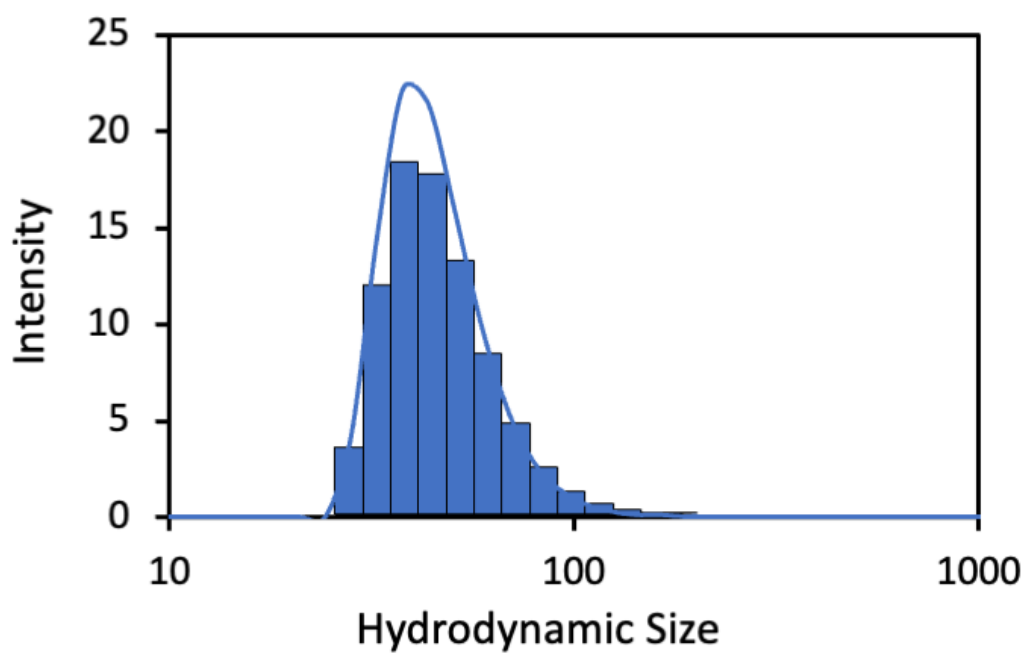


Figure S3. The hydrodynamic diameter of the prepared chemiluminescence Q842 nanoparticles.

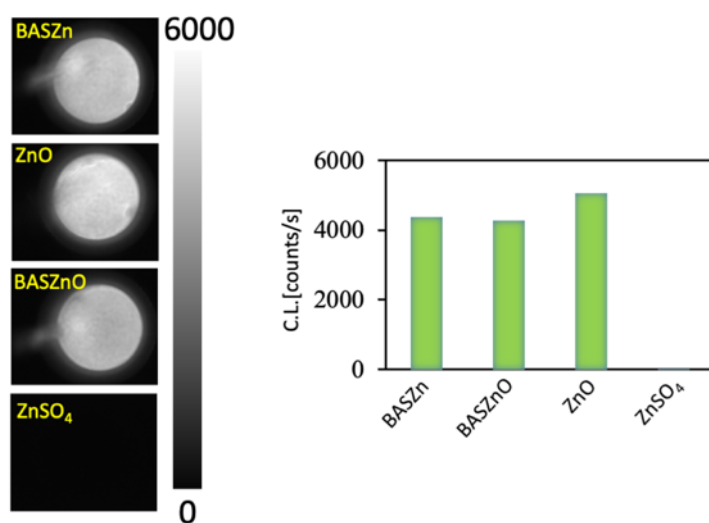


Figure S4. The chemiluminescence of Q842 nanoparticles in the presence of BSAZn, BSAZnO, ZnO nanoparticles and ZnSO₄. Exposure time 1s, 1000 nm long pass filter, Q842 nanoparticle (Q842 0.4 mg/mL, CPPO 1 mg/mL), H₂O₂ 100 mM, molar concentration of Zn about 18 mM for BSAZn, BSAZnO, ZnO and Zn²⁺.

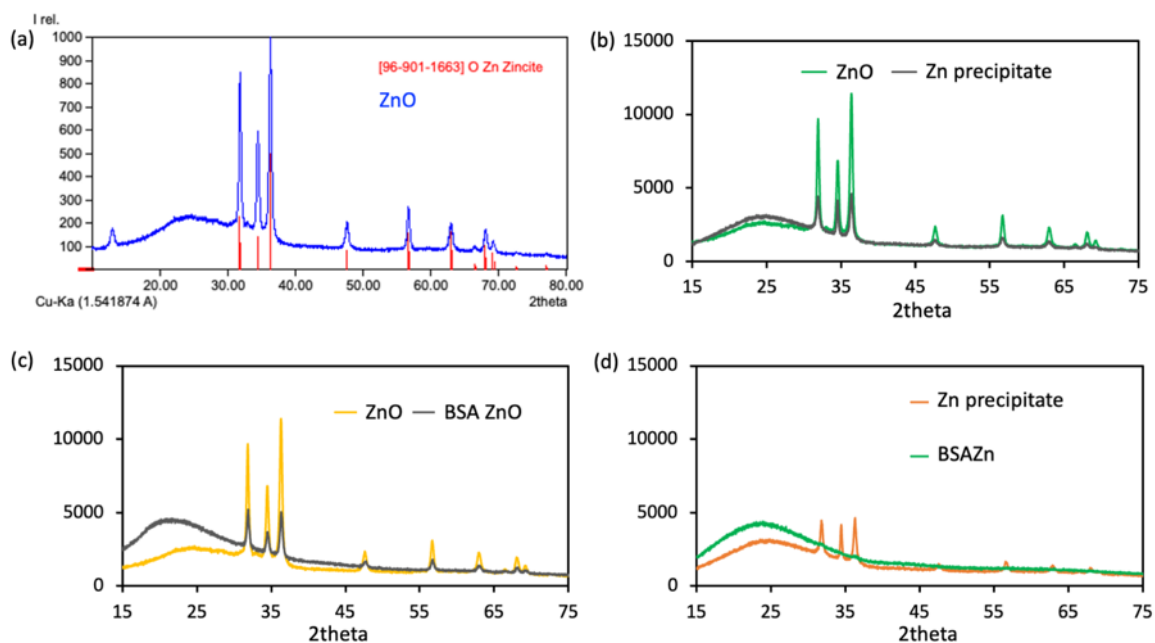


Figure S5. (a) The XRD of ZnO nanoparticles (blue curve), the red vertical lines are the XRD of Zincite crystal. (b) The XRD of the ZnO nanoparticle (green curve) and the ZnSO₄+NaOH precipitate (gray). (c) The XRD of the ZnO nanoparticle (orange curve) and the BSA complex BSAZnO (gray). (d) The XRD of the ZnSO₄+NaOH precipitate (orange curve) and the corresponding BSA complex BSAZn (green).

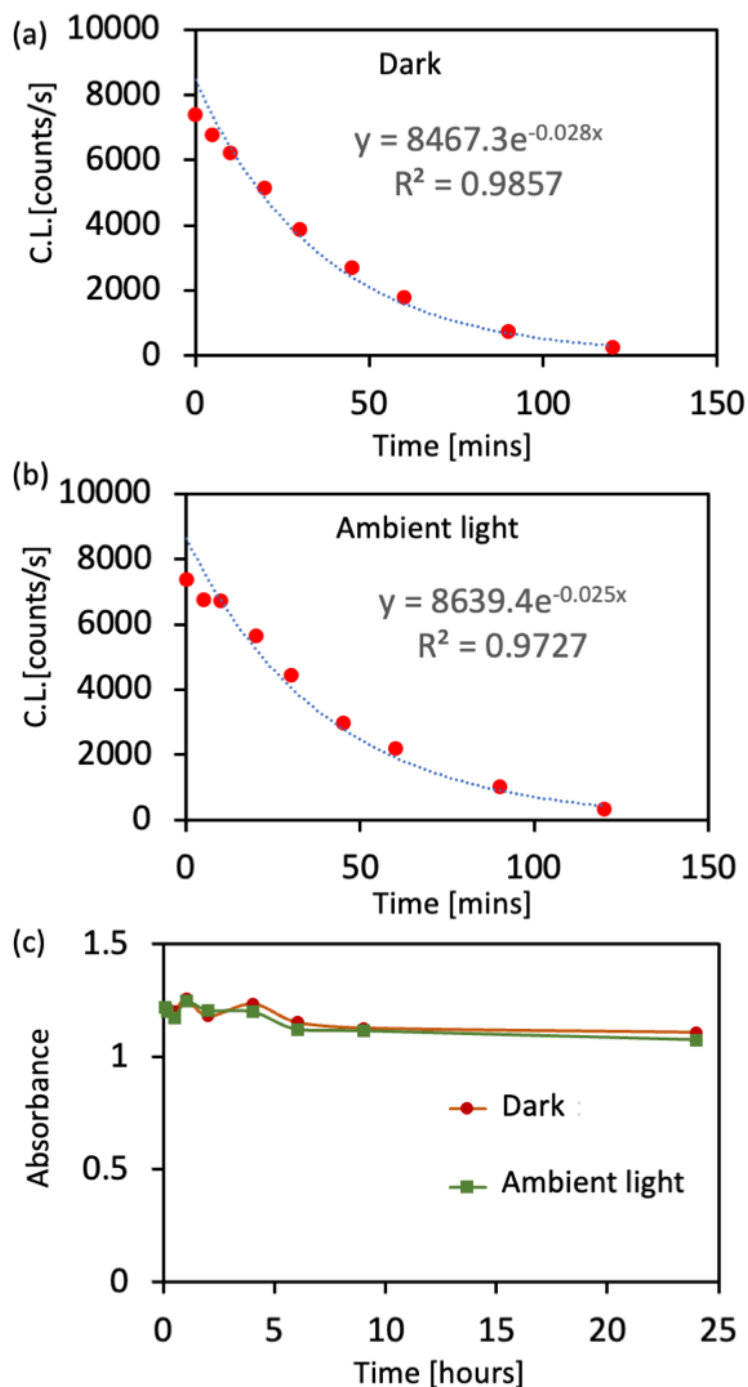


Figure S6. The CPPO stability in the Q842 C.L. nanosystem at 37 °C, Exposure time 1s, 900 nm long pass filter, Q842 nanoparticle (Q842 0.1 mg/mL, CPPO 1 mg/mL), H₂O₂ 100 mM, molar concentration of Zn about 18 mM for BSAZn. **(a)** The chemiluminescence of the Q842 nanosystem as a function of incubation time in dark. **(b)** The chemiluminescence of the Q842 nanosystem as a function of incubation time at ambient light. **(c)** The normalized absorption intensity of Q842 nanosystem at 825 nm as a function of incubation time in dark.

We may find that there is no significant variation on the absorbance of Q842. It indicates that during the incubation time interval, the Q842 concentration does not change. The Chemiluminescence intensity decay comes from the self-decomposition of the CPPO.

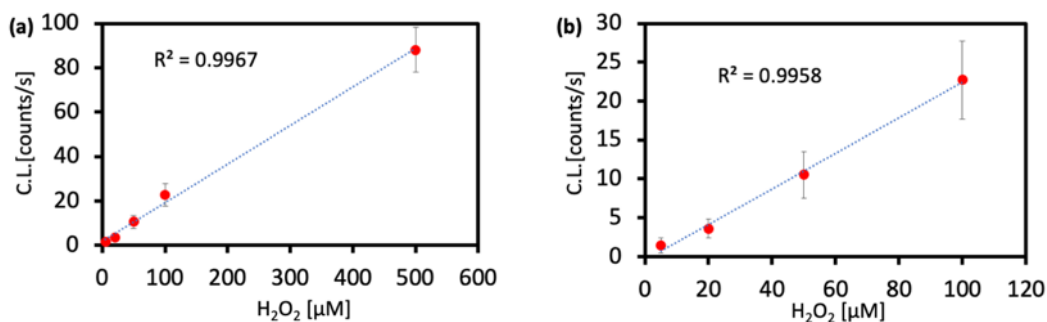


Figure S7. The chemiluminescence intensity of Q842 as a function of H_2O_2 concentration. Exposure time 1s, 900 nm long pass filter, Q842 nanoparticle (Q842 0.4 mg/mL, CPPO 1 mg/mL), molar concentration of Zn about 18 mM for BSAZn.

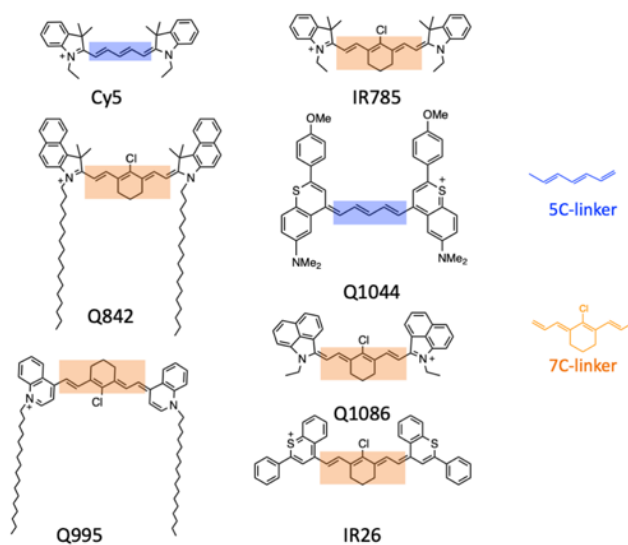


Figure S8. Molecular structures of the investigated dyes.

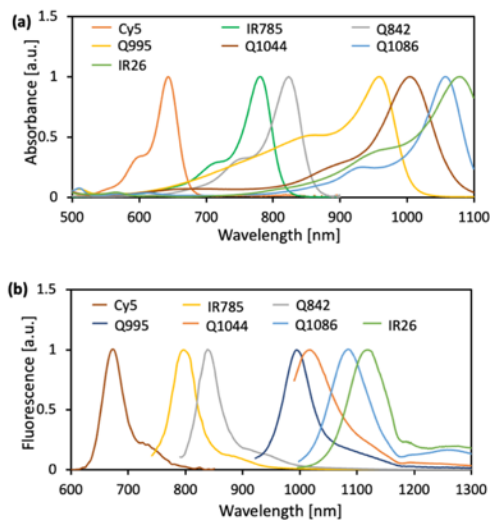


Figure S9. (a) The absorption spectra of investigated dyes in a solution of THF with 10% of H_2O . (b) The emission spectra of investigated dyes in a solution of THF with 10% of H_2O .

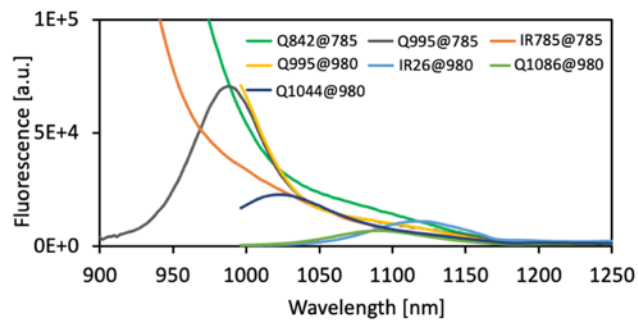


Figure S10. The fluorescent spectra of investigated dyes with 900 nm long pass filter, with absorbance around 0.1 at the excitation wavelength.

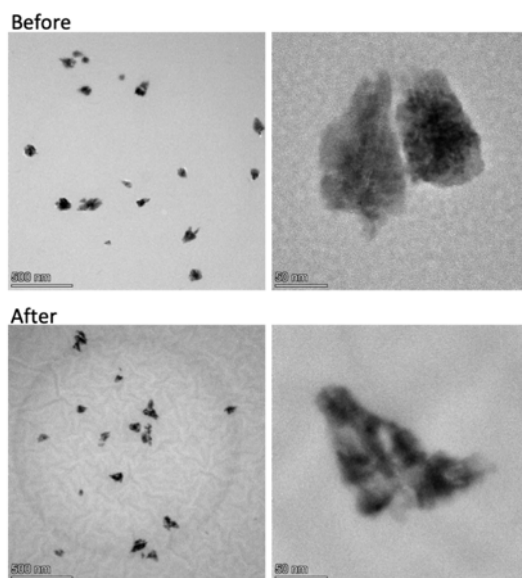


Figure S11. The TEM image of BSAZn before and after the CL experiment.

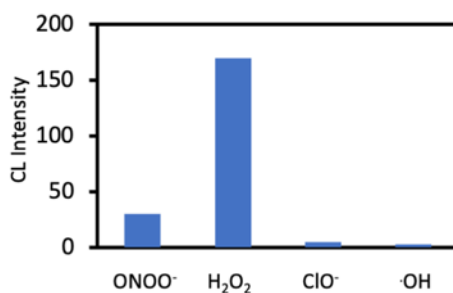


Figure S12. The selectivity of the CL nanosystem in the presence of ONOO•, •OH and ClO• and H₂O₂ at concentration about 1.5 mM with 900 nm longpass filter and the intensity was averaged for 10 s. Q842 nanoparticle (Q842 0.2mg/mL, CPPO 1 mg/mL), molar concentration of Zn about 18 mM for BSAZn.

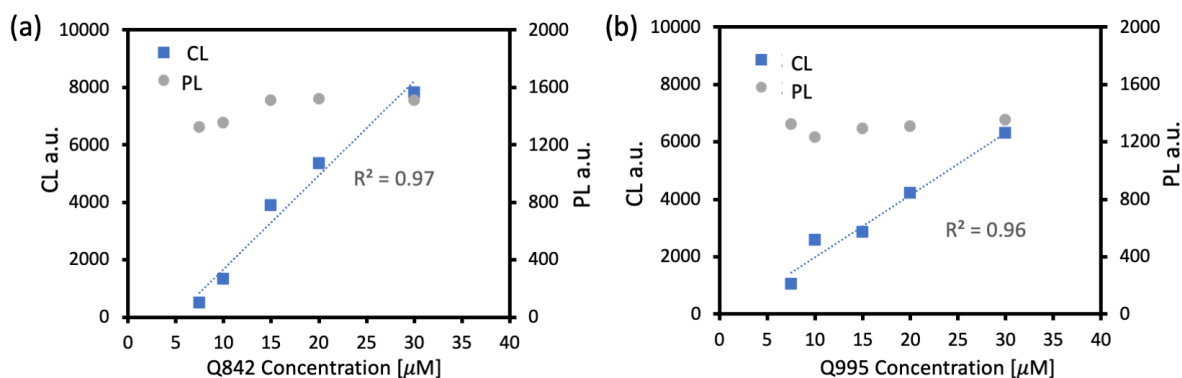


Figure S13. The CL and PL intensity variation as a function of dye concentration. For PL experiments, the excitation wavelength at 785 nm, 5 mW, optical length about 1 cm. For CL experiments, the H_2O_2 , CPPO and dye molar ratio was constant for all concentration conditions. (a) The CL and PL intensity variation as a function of Q842 concentration. (b) The CL and PL intensity variation as a function of Q995 concentration.

Due to the relatively low photon flux of the CL experiments, the dye concentration can not be taken as low as that in PL linear region. For instance, Q842 with ϵ_{CL} about from 1 to 5, ϵ about $170,000 \text{ M}^{-1}\text{cm}^{-1}$, L around 1 cm, the relation between fluorescence intensity and dye concentration is far away from the linear region according to Lambert-Beer's Law. However, for the case of CL intensity, as long as the molar ratio of H_2O_2 , CPPO and dye keep constant, the CL intensity would be linearly response to the dye concentration.

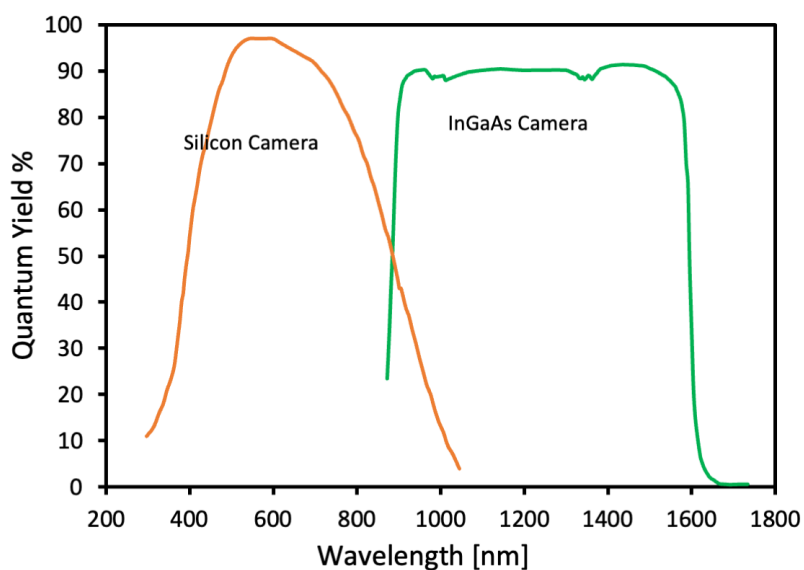


Figure S14. The spectral response of typical silicon camera and the InGaAs camera used in present work as a function of wavelength.

Table S1. The HOMO and LUMO energy of investigated dyes and the DOD.

Name	LUMO (ev)	HOMO (ev)	LUMO _{DOD} -HOMO _{Dye}
DOD	-4.142	-9.594	-
Cy5	-5.515	-7.911	3.77
IR785	-5.540	-7.563	3.42
Q842	-5.414	-7.347	3.21
Q995	-5.351	-7.061	2.92
Q1044	-5.814	-7.085	2.94
Q1086	-5.839	-7.432	3.29
IR26	-6.222	-7.819	3.68

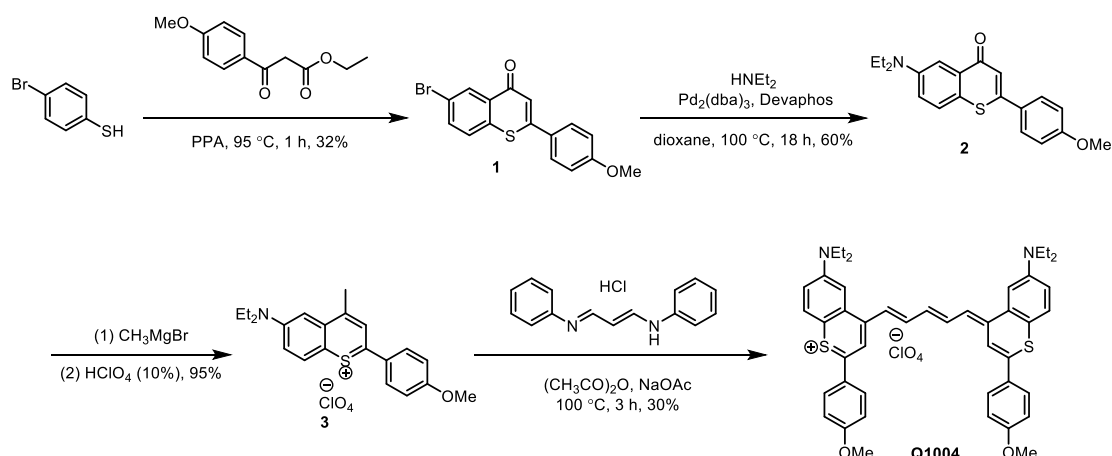
Table S2. The Calculated energy of DOD, DOD@Ts, DOD@D and CO₂. The total energy of CO₂ is doubled as the dissociation of one molecule of DOD produces two molecules of CO₂

eV	DOD	DOD@Ts	DOD@D	CO ₂
LUMO	-4.14	-8.48	-4.82	-0.19
HOMO	-9.59	-10.02	-10.50	-10.30
Total Energy	0	1.1	-2.2	-4.7

Table S3. The experimental details in Figure 3 and Figure 5

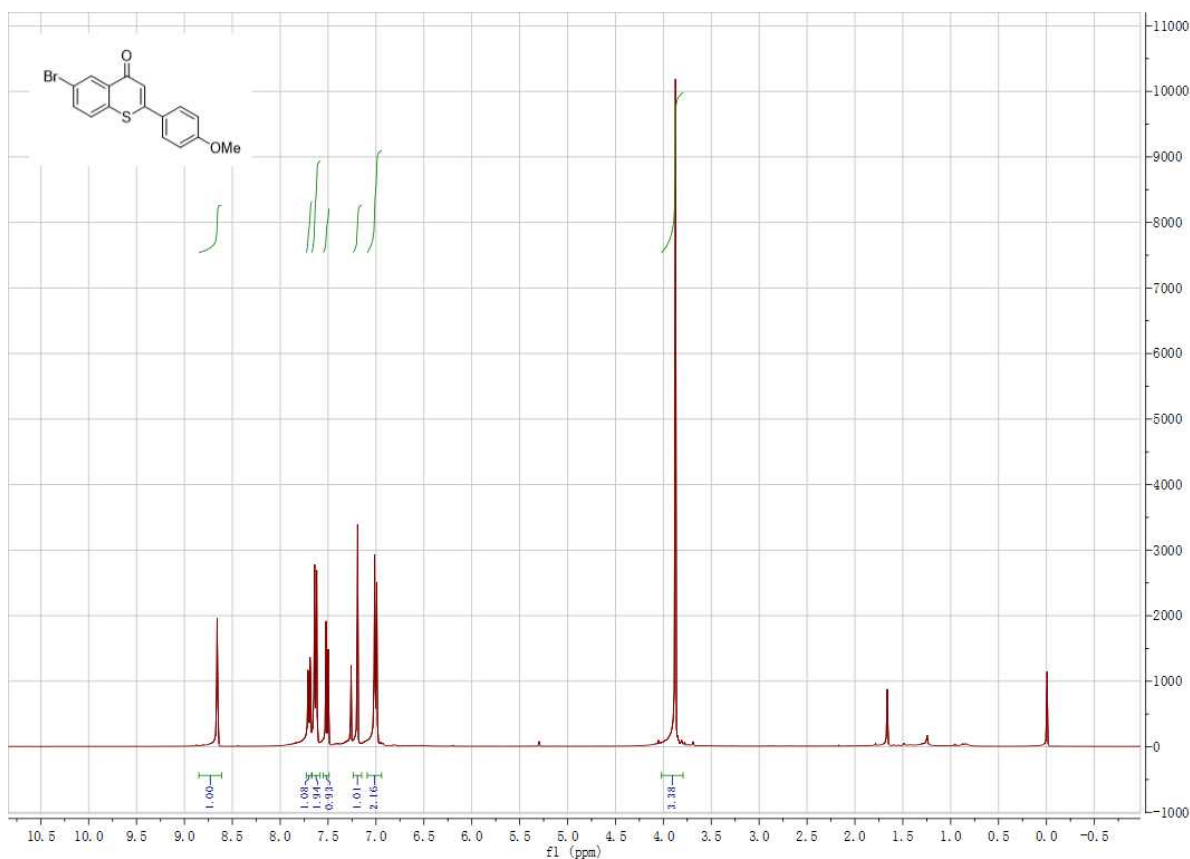
Figure 1d. Q842 100 $\mu\text{g/ml}$, BSAZn 18 mM, H ₂ O ₂ 50 mM, exposure time 1s.	Figure 1e. Q995 100 $\mu\text{g/ml}$, BSAZn 18 mM, H ₂ O ₂ 50 mM, exposure time 1s.
Figure 1g. Q842 100 $\mu\text{g/ml}$, BSAZn 18 mM, H ₂ O ₂ 10 mM, 900 nm long pass, exposure time 1s.	Figure 1h. Q842 100 $\mu\text{g/ml}$, BSAZn 18 mM, 900 nm long pass, exposure time 1s.
Figure 4a. Exposure time 1s, 900 nm long pass filter, Q842 400 $\mu\text{g/ml}$ of C.L. nanoparticle, BSAZn 18 mM, GOx 10 mg/mL.	Figure 4d. BSAZn nanoenzyme (18 mM), 100 μL of (Q842 400 $\mu\text{g/mL}$ of C.L. nanoparticle, GOx 10 mg/mL, glucose 100mM).
Figure 4e. 10 μL 1 M H ₂ O ₂ , with exposure time 1 s and 100 μL of (Q842 400 $\mu\text{g/mL}$ of C.L. nanoparticle, BSAZn 18 mM).	

Synthesis of Q1044

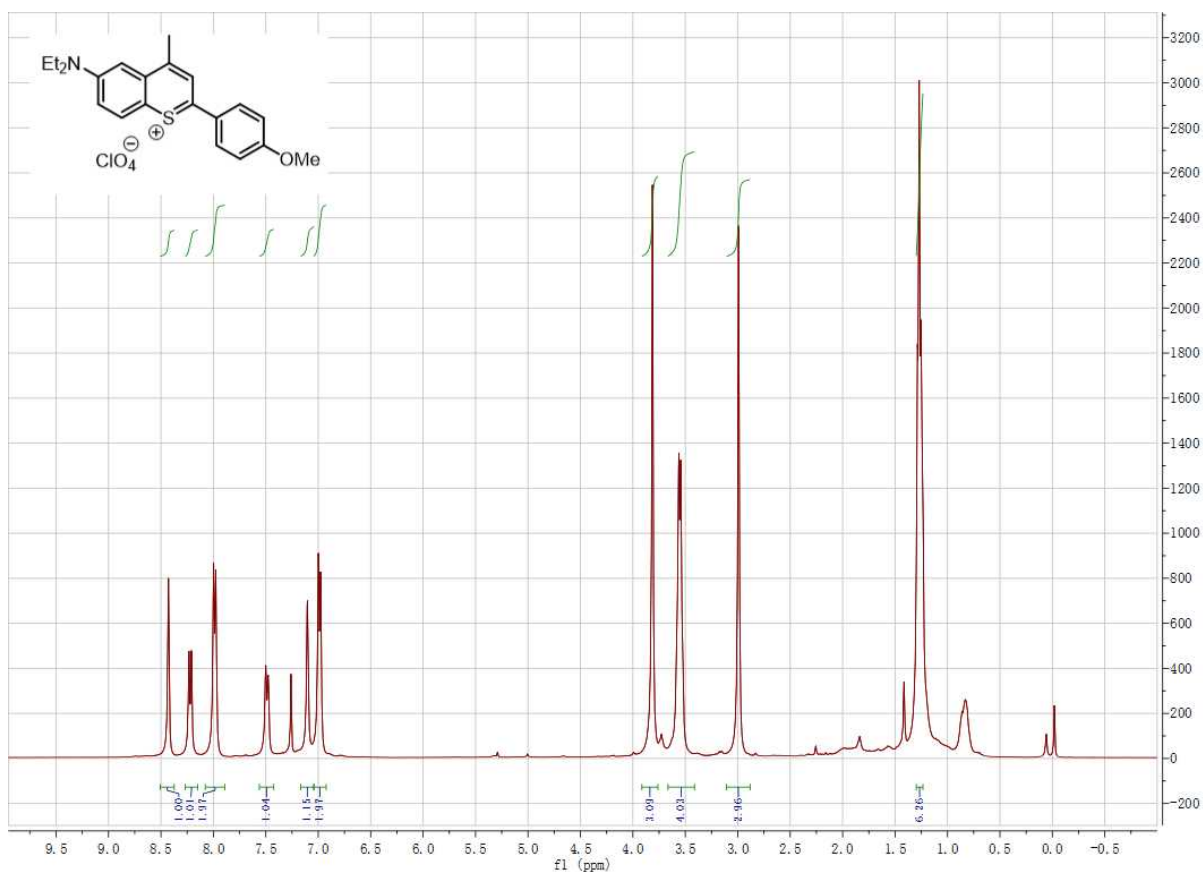


6-bromo-2-(4-methoxyphenyl)-4H-thiopyridin-4-one 1:

To a hot polyphosphoric acid (PPA, 10 mL), ethyl 3-(4-methoxyphenyl)acrylate (2.6 g, 11.7 mmol) and 4-bromobenzenethiol (2.0 g, 10.6 mmol) were added gradually, the mixture was stirred vigorously at 95 °C for 1 h. After cooling to room temperature, ice water was added slowly to quench the reaction and extracted with CH₂Cl₂ (3 times). The combined organic extracts were dried on Na₂SO₄, the solvent was evaporated. The crude product was further purified by a flash column chromatography (Petroleum ether/CH₂Cl₂, 50/50 to 0/100) on silica gel to give the compound **1** (1.18 g, 32%). ¹H NMR (400 MHz, CDCl₃) δ 8.66 (d, *J* = 2.0 Hz, 1H), 7.70 (dd, *J* = 2.0, 8.5 Hz, 1H), 7.63 (d, *J* = 8.8 Hz, 2H), 7.51 (d, *J* = 8.5 Hz, 1H), 7.19 (s, 1H), 7.00 (d, *J* = 8.8 Hz, 2H), 3.87 (s, 3H).

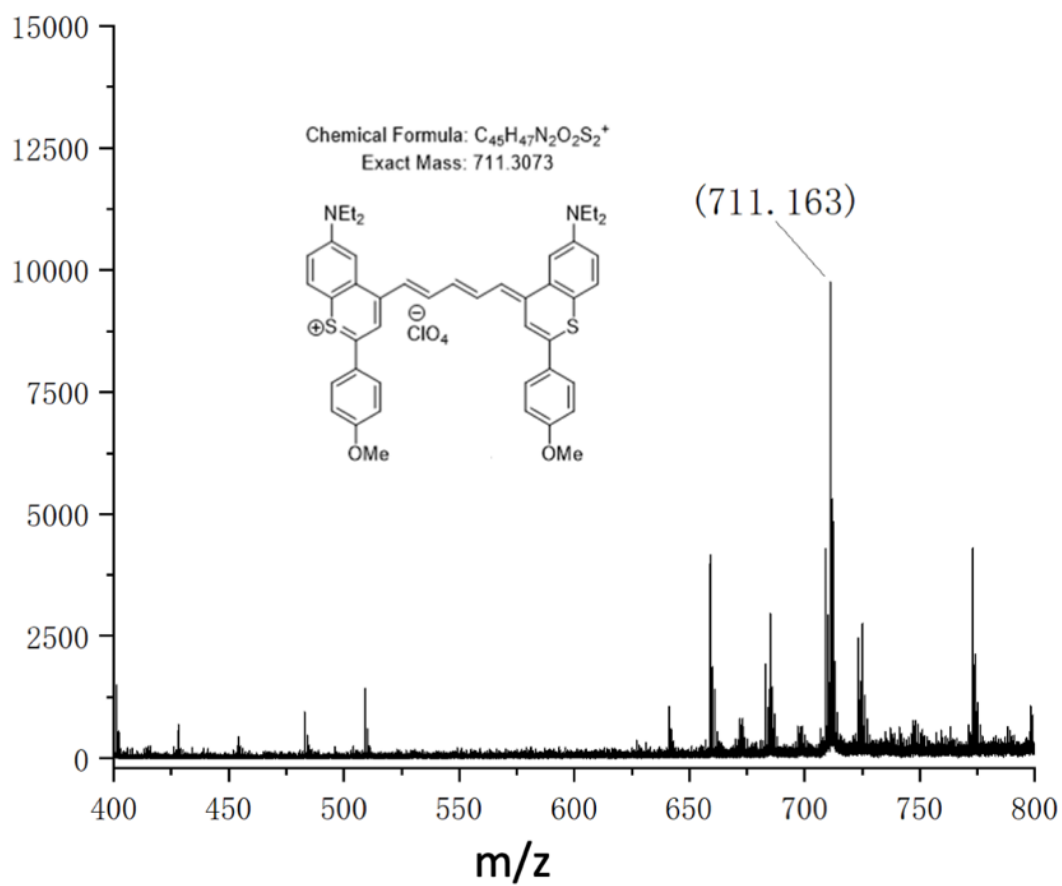
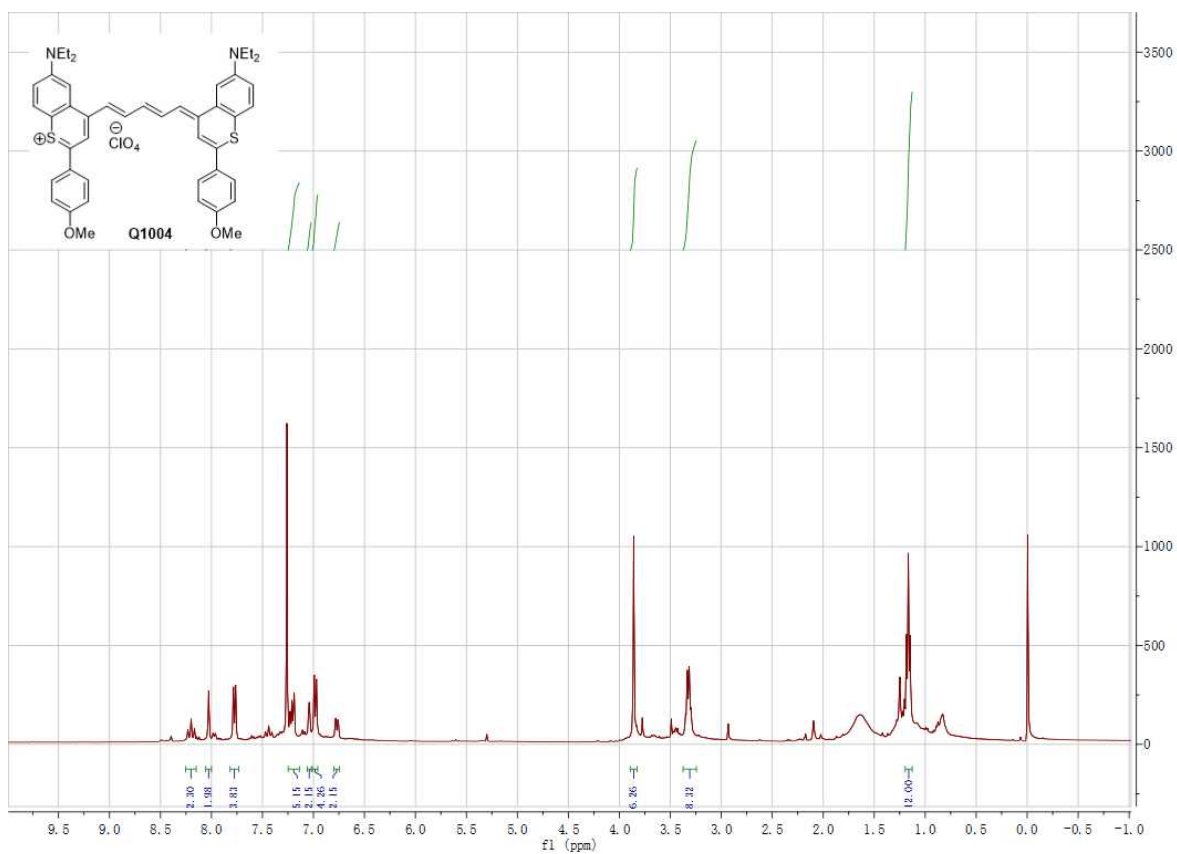


6-(diethylamino)-2-(4-methoxyphenyl)-4H-thiopyridin-4-one 2:

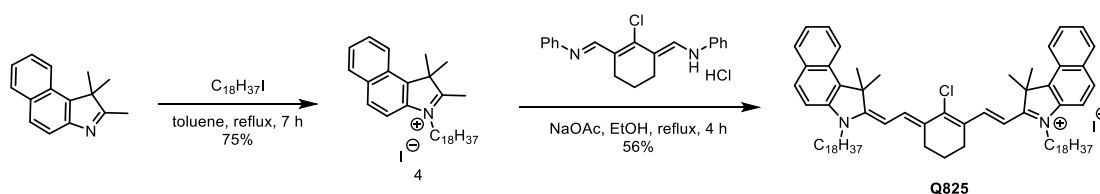


6-(diethylamino)-4-((1*E*,3*E*)-5-((*E*)-6-(diethylamino)-2-(4-methoxyphenyl)-4*H*-thiochromen-4-ylidene)penta-1,3-dien-1-yl)-2-(4-methoxyphenyl)thiochromenylium perchlorate Q1044:

To a mixture of compound **3** (66 mg, 0.15 mmol), *N*-((1*E*,3*E*)-3-(phenylimino)prop-1-en-1-yl)aniline hydrochloride (19.5 mg, 0.075 mmol), NaOAc (12.3 mg, 0.15 mmol), anhydrous Ac₂O (0.3 mL) and anhydrous acetonitrile (0.6 mL) were added in a sequence. The mixture was heated at 100 °C under nitrogen for 3 h. After cooling to room temperature, the mixture was evaporated and purified by a column chromatography (MeOH/CH₂Cl₂, 0/100 to 1/99) on silica gel to give afforded **Q1044** (37 mg, 30%). ¹H NMR (400 MHz, CDCl₃) δ 8.20 (t, *J* = 12.9 Hz, 2H), 8.03 (s, 2H), 7.77 (d, *J* = 8.6 Hz, 4H), 7.35-7.16 (m, 5H), 7.14 (s, 2H), 6.98 (d, *J* = 8.6 Hz, 4H), 6.77 (m, 2H), 3.86 (s, 6H), 3.32 (q, *J* = 6.8 Hz, 8H), 1.17 (t, *J* = 6.8 Hz, 12H). HRMS (MALDI-TOF) *m/z*: [M-ClO₄]⁺ calcd for C₄₅H₄₇N₂O₂S₂⁺: 711.307; Found: 711.163.



Synthesis of Q842

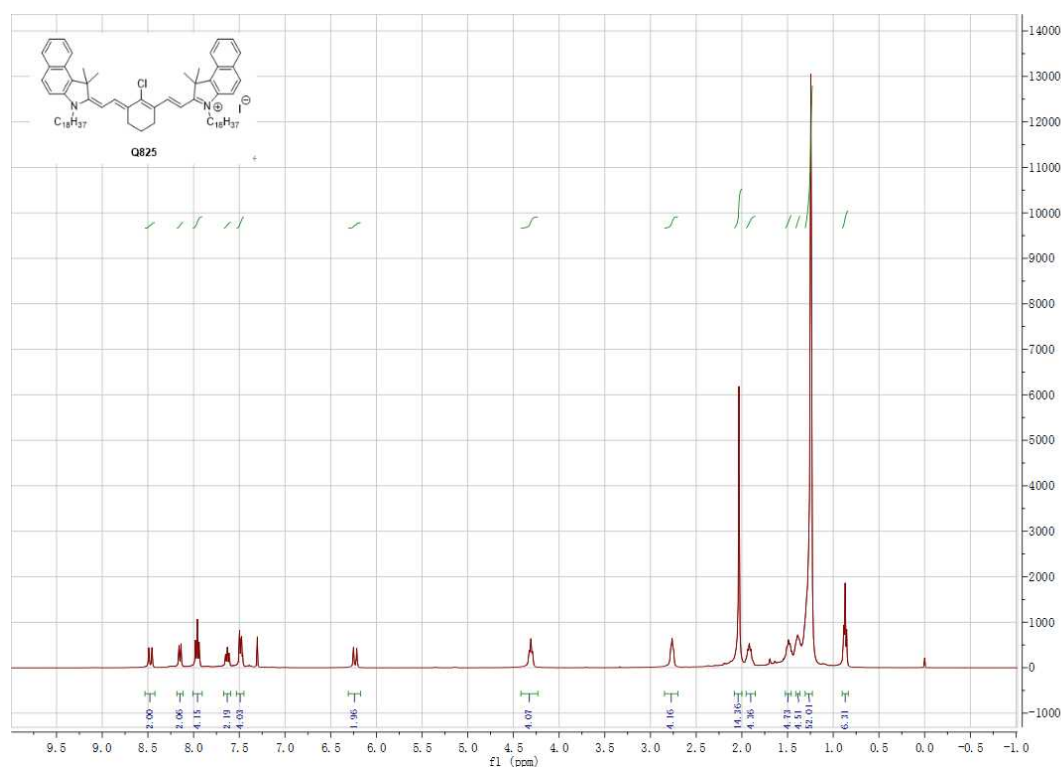


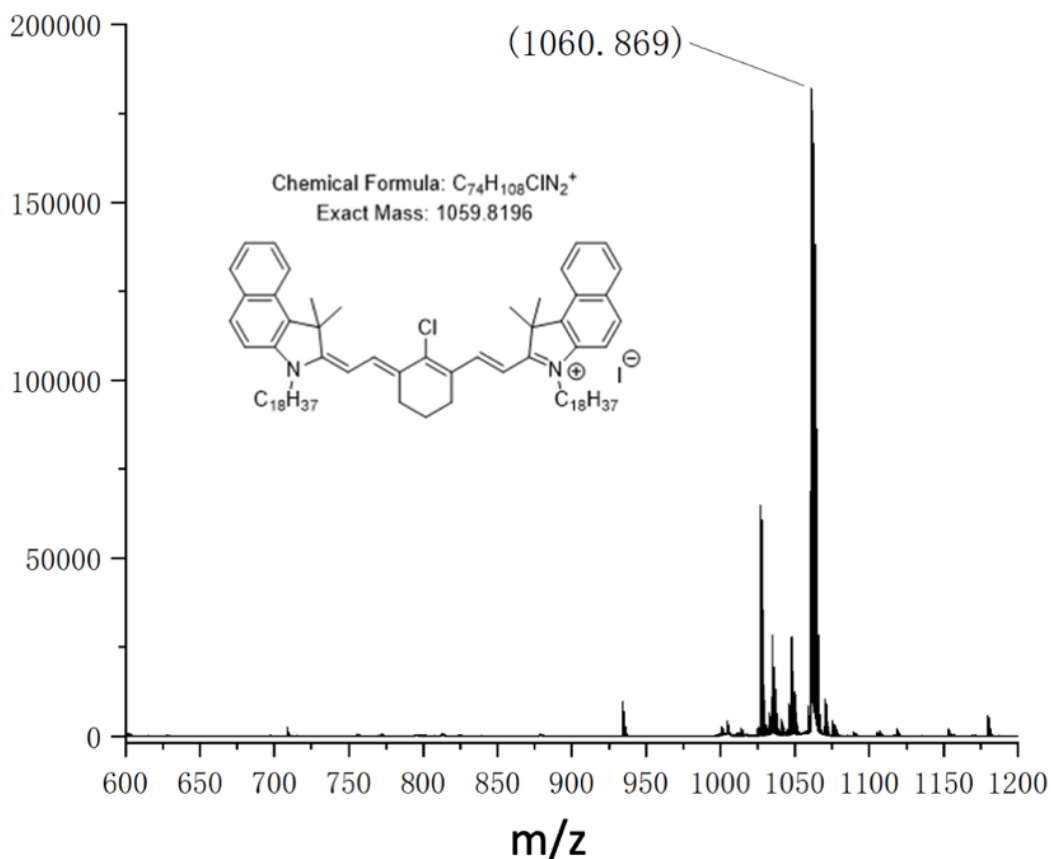
1,1,2-trimethyl-3-octadecyl-1H-benzo[e]indol-3-ium iodide 4:

To a solution of 1,1,2-trimethyl-1H-benzo[e]indole (1.25 g, 6.0 mmol) in toluene (10 mL), $C_{18}H_{37}I$ (2.74 g, 7.2 mmol) was added under argon atmosphere. The reaction mixture was stirred under reflux for 7 h, then allowed to cool to room temperature. The solvent was removed under vacuum filtration and the residue was washed with ether to afford the desired product **4** (2.65 g, 75%), which was used for the next step without further purification.

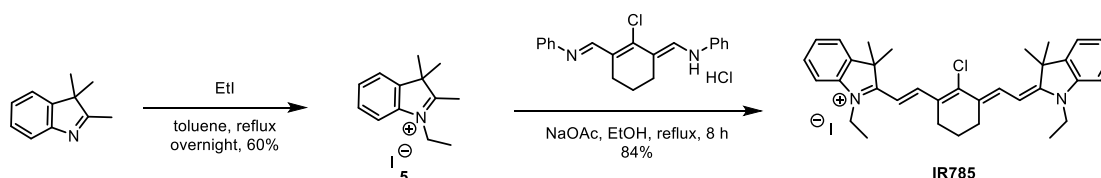
2-((E)-2-((E)-2-chloro-3-((E)-2-(1,1-dimethyl-3-octadecyl-1,3-dihydro-2H-benzo[e]indol-2-

ylidene)ethylidene)cyclohex-1-en-1-yl)vinyl)-1,1-dimethyl-3-octadecyl-1H-benzo[e]indol-3-ium iodide **Q842**: To a solution of compound **4** (1.18 g, 2.0 mmol) in EtOH (40 mL), sodium acetate (164 mg, 2.0 mmol) and *N*-((*E*)-2-chloro-3-((*E*)-(phenylimino)methyl)cyclohex-2-en-1-ylidene)methyl)aniline hydrochloride (359 mg, 1.0 mmol) was added gradually under argon atmosphere. The reaction mixture was stirred under reflux for 4 h, then allowed to cool to room temperature. After evaporation of solvent, the residue was purified by flash chromatography (MeOH/acetone/ CH_2Cl_2 , 2.5/12.5/85) to afford **Q842** (660 mg, 56%) as a green solid. 1H NMR (400 MHz, $CDCl_3$) δ 8.47 (d, $J = 14.1$ Hz, 2H), 8.15 (d, $J = 8.5$ Hz, 2H), 7.96 (app. t, $J = 8.2$ Hz, 4H), 7.67-7.59 (m, 2H), 7.52-7.44 (m, 4H), 6.23 (d, $J = 14.1$ Hz, 2H), 4.31 (t, $J = 7.0$ Hz, 4H), 2.76 (t, $J = 5.4$ Hz, 4H), 2.10-2.00 (m, 14H), 1.95-1.85 (m, 4H), 1.54-1.45 (m, 4H), 1.42-1.35 (m, 4H), 1.32-1.22 (m, 52H), 0.87 (t, $J = 6.7$ Hz, 6H). HRMS (MALDI-TOF) m/z : $[M-I]^+$ calcd for $C_{74}H_{108}ClN_2^+$: 1059.820; Found: 1060.869.





Synthesis of IR785



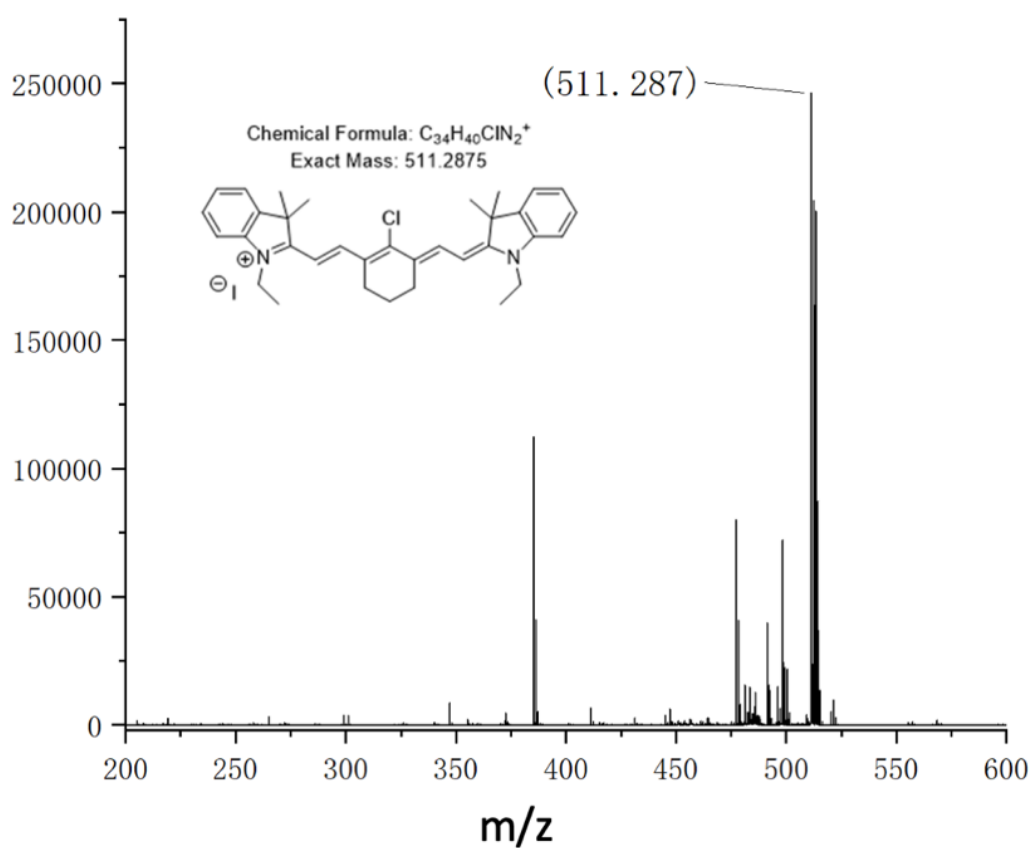
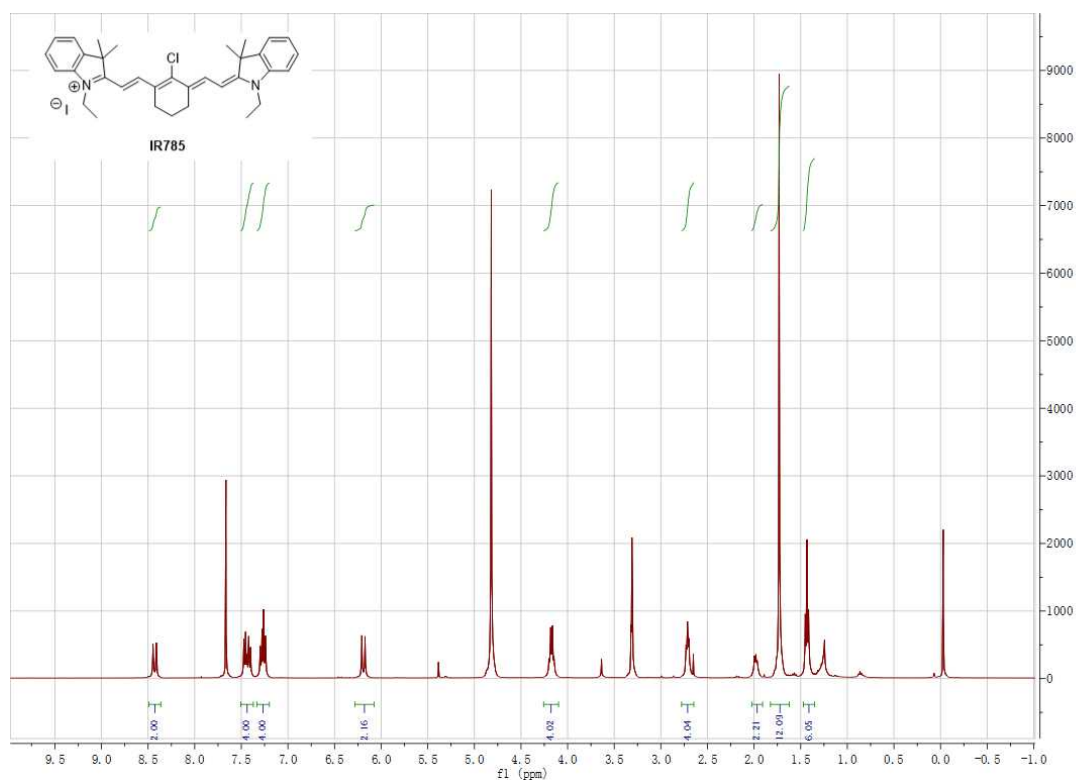
1-ethyl-2,3,3-trimethyl-3H-indol-1-ium iodide 5:

To a solution of 2,3,3-trimethyl-3H-indole (1.59 mL, 10.0 mmol) in toluene (20 mL), C_2H_5I (1.2 mL, 15.0 mmol) was added under argon atmosphere. The reaction mixture was stirred under reflux for overnight, then allowed to cool to room temperature. The solvent was removed under vacuum filtration and the residue was washed with ether to afford the desired product **5** (1.88 g, 60%) as a pink solid, which was used for the next step without further purification.

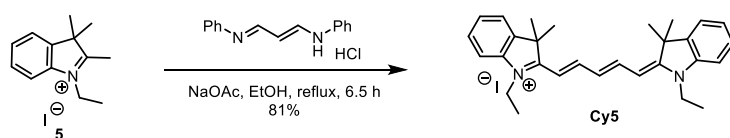
2-((E)-2-((E)-2-chloro-3-((E)-1-ethyl-3,3-dimethylindolin-2-ylidene)ethylidene)cyclohex-1-en-1-ylvinyl)-1-ethyl-3,3-dimethyl-3H-indol-1-ium iodide IR785:

To a solution of compound **5** (283 mg, 0.90 mmol) in EtOH (5.0 mL), sodium acetate (148 mg, 1.8 mmol) and *N*-((E)-2-chloro-3-((E)-(phenylimino)methyl)cyclohex-2-en-1-ylidene)methyl)aniline hydrochloride (161 mg, 0.45 mmol) was added gradually under argon atmosphere. The reaction mixture was stirred under reflux for 8 h, then allowed to cool to room temperature. After evaporation of solvent, the residue was purified by flash

chromatography (MeOH /CH₂Cl₂, 1/20) to afford **IR785** (242 mg, 84%) as a green solid. ¹H NMR (400 MHz, MeOD-CDCl₃) δ 8.43 (d, *J* = 14.1 Hz, 2H), 7.50-7.36 (m, 4H), 7.28 (app. t, *J* = 7.5 Hz, 2H), 7.25 (d, *J* = 7.9 Hz, 2H), 6.19 (d, *J* = 14.1 Hz, 2H), 4.17 (q, *J* = 7.1 Hz, 4H), 2.71 (t, *J* = 5.7 Hz, 4H), 2.03-1.91 (m, 2H), 1.73 (s, 12H), 1.43 (t, *J* = 7.1 Hz, 6H). HRMS (MALDI-TOF) *m/z*: [M-I]⁺ calcd for C₃₄H₄₀ClN₂⁺: 511.288; Found: 511.287.

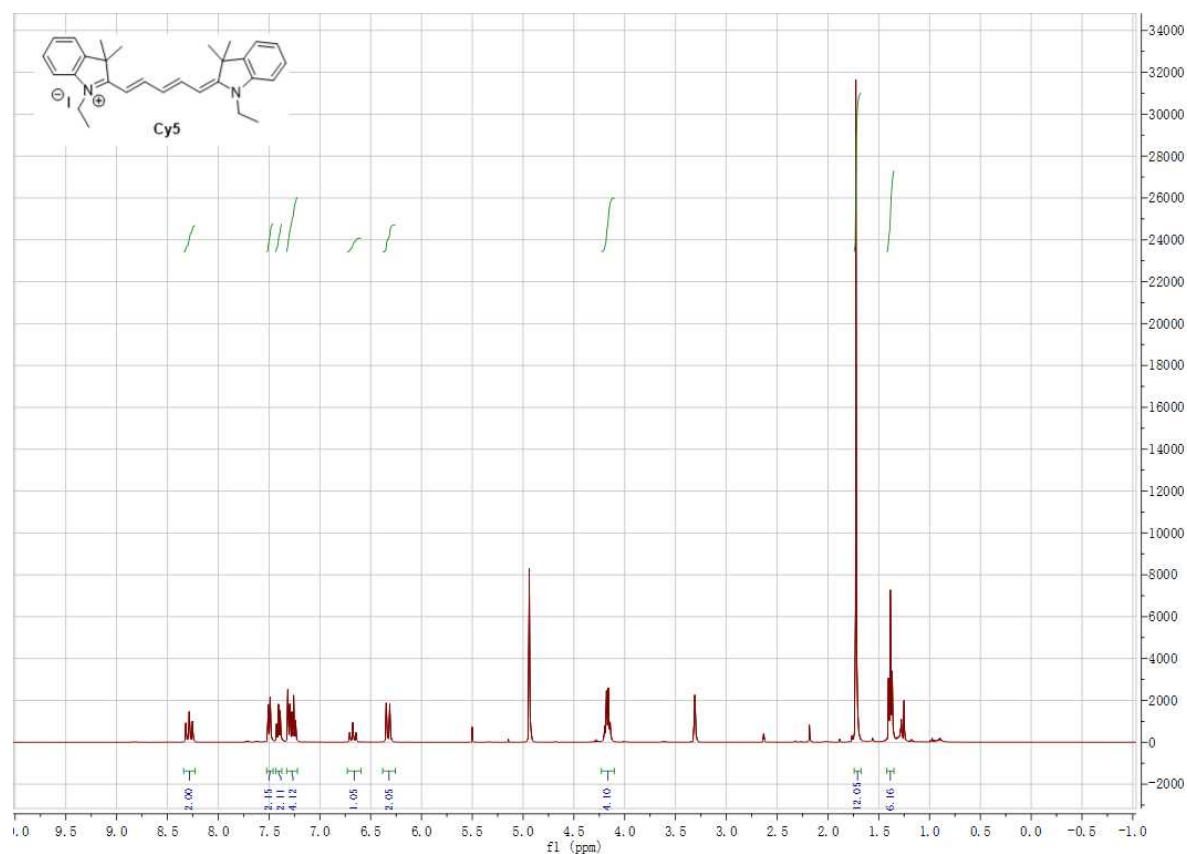


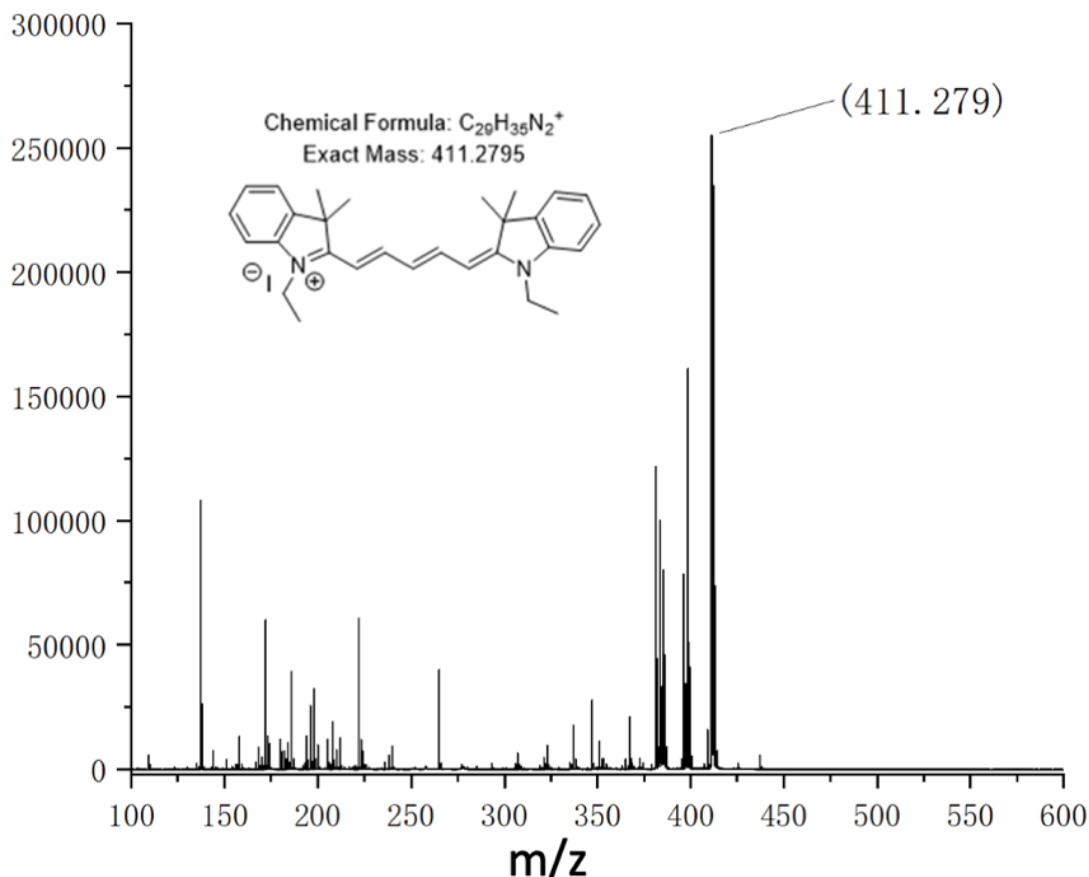
Synthesis of Cy5



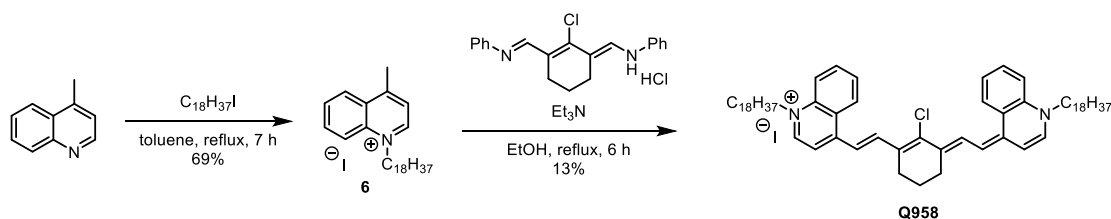
1-ethyl-2-((1E,3E)-5-((E)-1-ethyl-3,3-dimethylindolin-2-ylidene)penta-1,3-dien-1-yl)-3,3-dimethyl-3H-indol-1-ium iodide Cy5:

To a solution of compound **5** (315 mg, 1.0 mmol) in EtOH (5.0 mL), sodium acetate (164 mg, 2.0 mmol) and N-((1E,3E)-3-(phenylimino)prop-1-en-1-yl)aniline hydrochloride (129 mg, 0.50 mmol) was added gradually under argon atmosphere. The reaction mixture was stirred under reflux for 6.5 h, then allowed to cool to room temperature. After evaporation of solvent, the residue was purified by flash chromatography (EtOAc/CH₂Cl₂/Acetone, 10/5/5, then CH₂Cl₂/Acetone, 1/1) to afford **Cy5** (218 mg, 81%) as a blue solid. ¹H NMR (400 MHz, MeOD) δ 8.27 (t, J = 13.1 Hz, 2H), 7.49 (d, J = 7.3 Hz, 2H), 7.40 (dt, J = 12.5, 2.7 Hz, 2H), 7.33-7.22 (m, 4H), 6.68 (t, J = 12.5 Hz, 1H), 6.32 (d, J = 13.7 Hz, 2H), 4.17 (q, J = 7.2 Hz, 4H), 1.72 (s, 12H), 1.39 (t, J = 7.2 Hz, 6H). HRMS (MALDI-TOF) m/z: [M-I]⁺ calcd for C₂₉H₃₅N₂⁺: 411.280; Found: 411.279.





Synthesis of Q995



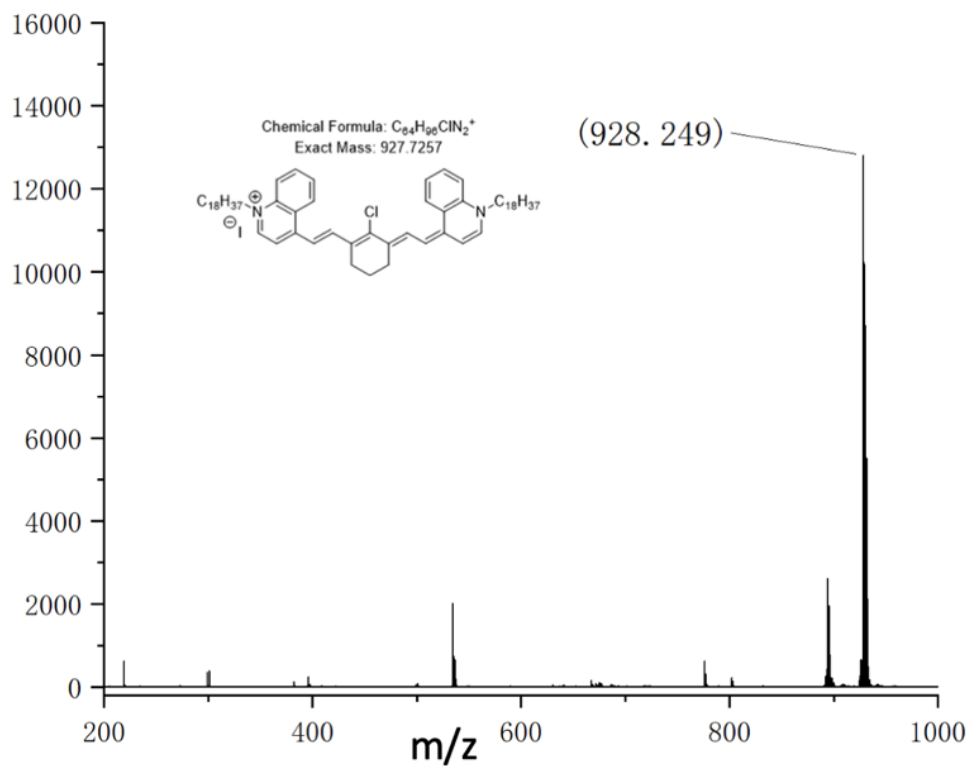
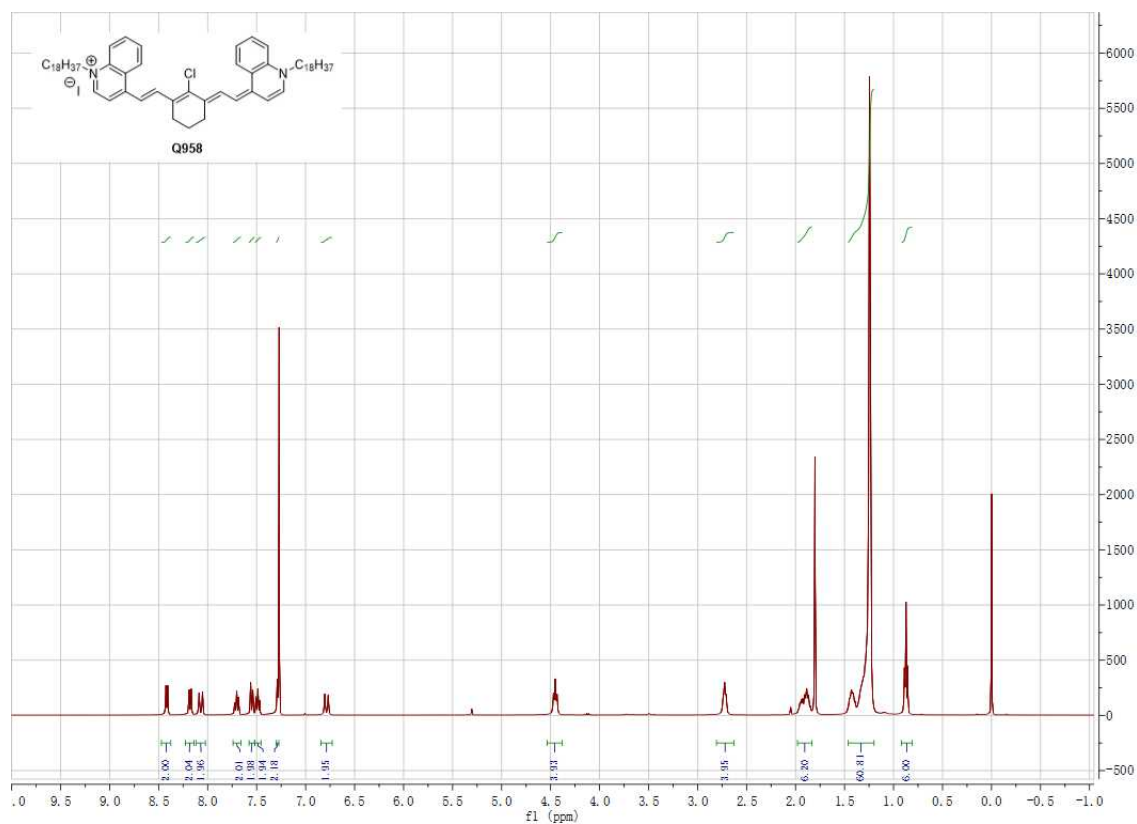
4-methyl-1-octadecylquinolin-1-ium iodide **6**:

To a solution of 4-methylquinoline (0.72 g, 5.0 mmol) in toluene (5.0 mL), $C_{18}H_{37}I$ (2.28 g, 6.0 mmol) was added under argon atmosphere. The reaction mixture was stirred under reflux for 7 h, then allowed to cool to room temperature. The solvent was removed under vacuum filtration and the residue was washed with ether to afford the desired product **6** (1.80 g, 69%) as a yellow solid, which was used for the next step without further purification.

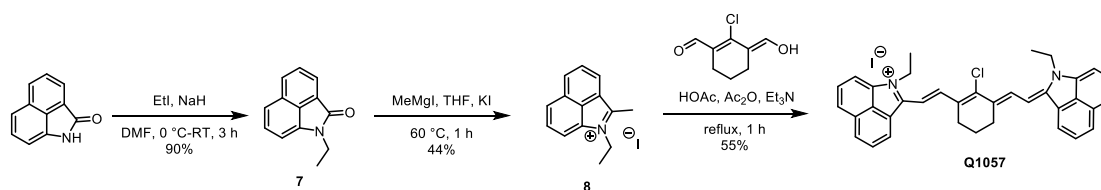
4-((*E*)-2-((*E*)-2-chloro-3-((*Z*)-1-octadecylquinolin-4(1*H*)-ylidene)ethylidene)cyclohex-1-en-1-yl)vinyl)-1-octadecylquinolin-1-ium iodide **Q995**:

To a solution of compound **6** (0.75 g, 1.43 mmol) in EtOH (50 mL), *N*-((*E*)-2-chloro-3-((*E*)-(phenylimino)methyl)cyclohex-2-en-1-ylidene)methyl)aniline hydrochloride (129 mg, 0.36 mmol) and Et_3N (0.93 mL, 6.5 mmol) was added gradually under argon atmosphere. The reaction mixture was stirred under reflux for 6 h, then allowed to cool to room temperature. After evaporation of solvent, the crude product was washed with acetone, the residue was purified by flash chromatography on neutral Al_2O_3 (MeOH / CH_2Cl_2 , 1/20) to afford **Q995** (137 mg, 13%) as a brown solid. 1H NMR (400 MHz, $CDCl_3$) δ 8.42 (d, $J = 7.2$ Hz, 2H), 8.18 (d, $J = 8.2$ Hz, 2H), 8.07

(d, $J = 13.8$ Hz, 2H), 7.70 (app. t, $J = 7.8$ Hz, 2H), 7.55 (d, $J = 8.7$ Hz, 2H), 7.49 (t, $J = 7.6$ Hz, 2H), 7.28 (d, $J = 7.2$ Hz, 2H), 6.79 (d, $J = 13.8$ Hz, 2H), 4.45 (t, $J = 7.3$ Hz, 4H), 2.72 (t, $J = 5.6$ Hz, 4H), 1.99-1.85 (m, 6H), 1.49-1.20 (m, 60H), 0.87 (t, $J = 6.8$ Hz, 6H). HRMS (MALDI-TOF) m/z : $[M-I]^+$ calcd for $C_{64}H_{96}ClN_2^+$: 927.726; Found: 928.249.



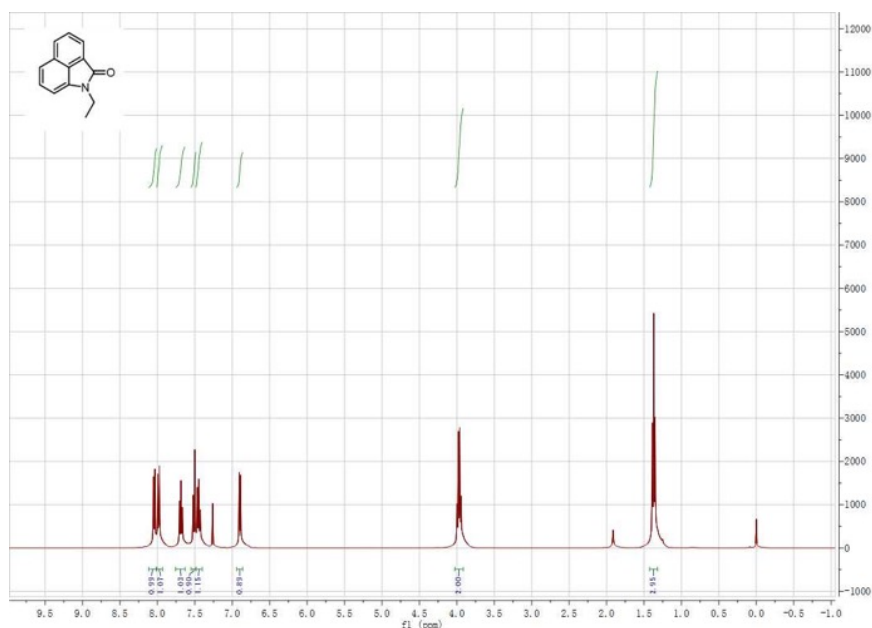
Synthesis of Q1086



The synthesis of Q1086 was according to reported literature with a bit modification ⁴.

1-ethylbenzo[cd]indol-2(1H)-one **7**:

NaH (60% dispersion in mineral oil, 1.20 g, 30 mmol) was added into a solution of benzo[cd]indol-2(1H)-one (1.69 g, 10 mmol) in 30 mL of anhydrous DMF under Ar atmosphere. Then the mixture was cooled to 0 °C, and EtI (0.96 mL, 12 mmol) was added dropwise. The mixture was stirred at room temperature for 3 h and then extracted with ethyl acetate. The organic phases were combined, washed with brine, dried over MgSO₄ and concentrated. The crude product was then purified by column chromatography on silica gel to give compound **7** (1.78 g, 90%) as a yellow solid. ¹H NMR (400 MHz, CDCl₃) δ 8.04 (d, *J* = 7.0 Hz, 1H), 7.98 (d, *J* = 8.1 Hz, 1H), 7.69 (t, *J* = 7.5 Hz, 1H), 7.51 (d, *J* = 8.4 Hz, 1H), 7.48-7.42 (m, 1H), 6.90 (d, *J* = 7.0 Hz, 1H), 3.97 (q, *J* = 7.2 Hz, 2H), 1.37 (t, *J* = 7.2 Hz, 3H).



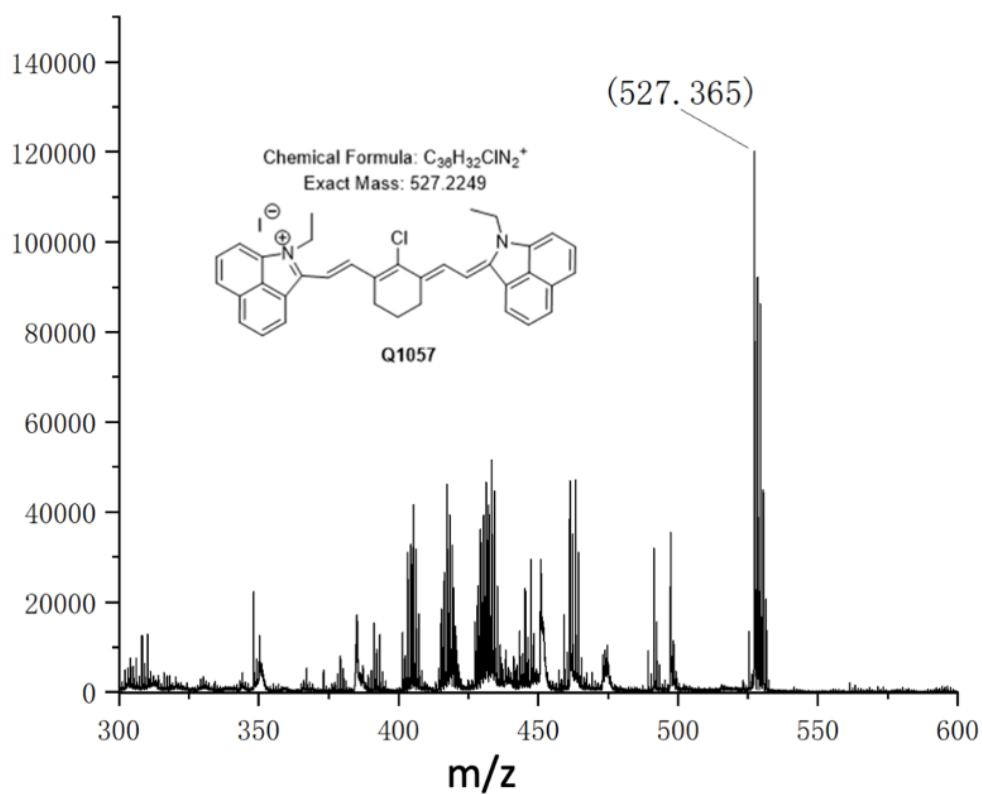
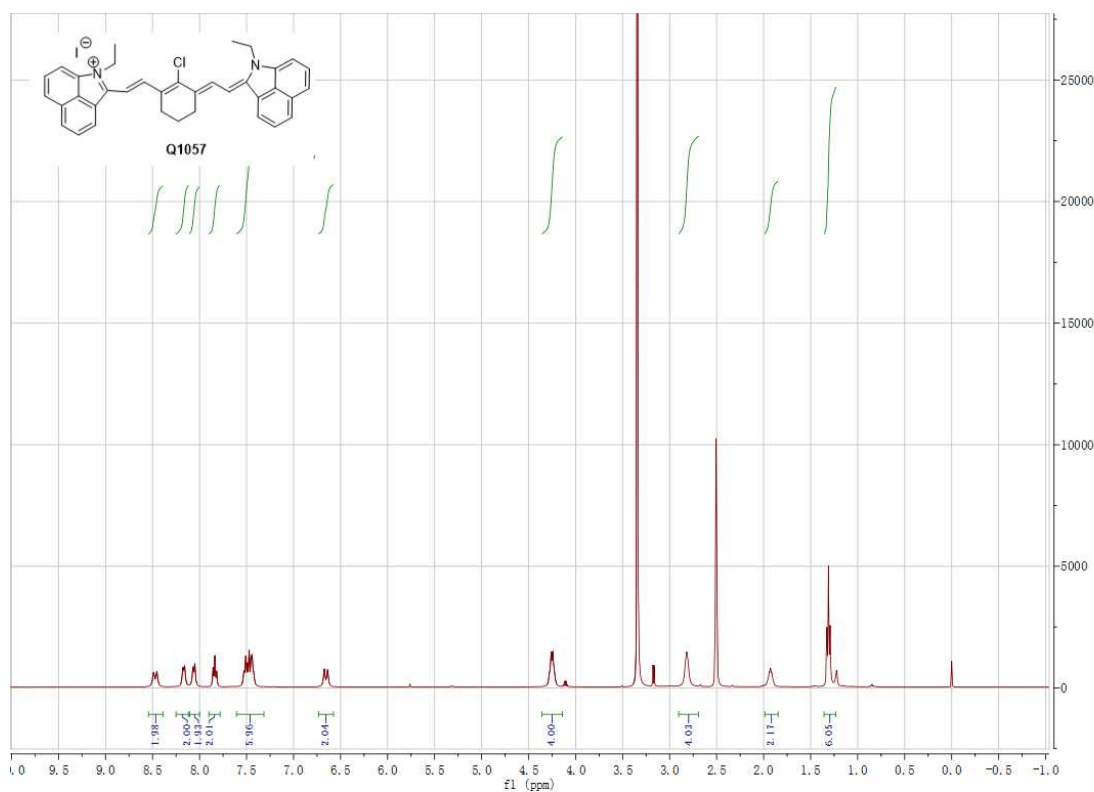
1-ethyl-2-methylbenzo[cd]indol-1-ium iodide **8**:

To a solution of **7** (1.78 g, 9.0 mmol) in 36 mL of anhydrous THF, MeMgBr (1 M solution in THF, 10.8 mL, 10.8 mmol) was added dropwise under Ar atmosphere. After stirring at 60 °C for 1 h, the mixture was cooled and hydrochloric acid (1 M, 15 mL) was added to the mixture. Then THF was evaporated, and NaI solution (1 M, 9 mL) was added to obtain red precipitate. The crude product was filtered, washed with water, ethyl acetate and acetone, then dried to give compound **8** (1.29 g, 44%) as red solid, which was used for the next step without further purification.

2-((E)-2-((E)-2-chloro-3-((Z)-2-(1-ethylbenzo[cd]indol-2(1H)-ylidene)ethylidene)cyclohex-1-en-1-yl)vinyl)-1-ethylbenzo[cd]indol-1-ium iodide **Q1086**:

To a solution of **8** (0.65 g, 2.0 mmol) and (E)-2-chloro-3-(hydroxymethylene)cyclohex-1-ene-1-carbaldehyde (0.17 mg, 1.0 mmol) in 2 mL of acetic acid, 1.0 mL of Et₃N and 1.0 mL of acetic anhydride were added and reacted at

60 °C for 30 min. Then the mixture was cooled, and 10 mL of ethyl acetate was added. The black precipitate was filtered and recrystallized in EtOH to give **Q1086** (0.54 g, 82%). $^1\text{H NMR}$ (400 MHz, DMSO- d_6) δ 8.47 (d, $J = 13.7$ Hz, 2H), 8.17 (d, $J = 6.9$ Hz, 2H), 8.06 (d, $J = 7.7$ Hz, 2H), 7.84 (app. t, $J = 7.7$ Hz, 2H), 7.56-7.40 (m, 6H), 6.66 (d, $J = 13.7$ Hz, 2H), 4.25 (q, $J = 7.0$ Hz, 4H), 2.86-2.78 (m, 4H), 1.98-1.86 (m, 2H), 1.31 (t, $J = 7.0$ Hz, 6H). HRMS (MALDI-TOF) m/z : $[\text{M-I}]^+$ calcd for $\text{C}_{36}\text{H}_{32}\text{ClN}_2^+$: 527.225; Found: 527.365.



Reference:

1. Becke, A. D. Density-functional thermochemistry. III. The role of exact exchange. *J. Chem. Phys* **98**, 5648–5652 (1993).
2. Lee, C., Yang, W. & Parr, R. G. Development of the Colle-Salvetti correlation-energy formula into a functional of the electron density. *Phys. Rev. B* **37**, 785–789 (1988).
3. Frisch, M. J.; Trucks, G. W.; Schlegel, H. B.; Scuseria, G. E.; Robb, M. A.; Cheeseman, J.R.; Scalmani, G.; Barone, V.; Mennucci, B.; Petersson, G. A.; Nakatsuji, H.; Caricato, M.; Li, X.; Hratchian, H. P.; Izmaylov, A. F.; Bloino, J.; Zheng, G.; Sonnenbe, D. J. Gaussian 16, Revision C.01,.
4. Feng, W.Q.; Zhang Y.Y.; Li, Z.; Zhai, S.Y.; Lv, W.J.; Liu, Z.H.. *Anal. Chem.* **2019**, *91*, 15757-15762.